Hindawi
Geofluids
Volume 2023, Article ID 6645245, 12 pages
https://doi.org/10.1155/2023/6645245

Research Article

The Effect of Slickwater on Shale Properties and Main Influencing Factors in Hydraulic Fracturing

Jiawei Liu,[1,2] **Xuefeng Yang**,[1,2] **Shengxian Zhao**,[1,2] **Yue Yang**,[1] **Shan Huang**,[1] **Lieyan Cao**,[1] **Jiajun Li**,[1] **and Jian Zhang**[1,2]

[1]*Shale Gas Research Institute, Southwest Oil & Gas Field Company, PetroChina, Chengdu, Sichuan 610051, China*
[2]*Shale Gas Evaluation and Exploitation Key Laboratory of Sichuan Province, Chengdu 610051, China*

Correspondence should be addressed to Jiawei Liu; jwliu_petrochina@163.com

Received 9 June 2023; Revised 21 October 2023; Accepted 28 November 2023; Published 18 December 2023

Academic Editor: Mohammad Sarmadivaleh

As shale gas reservoirs have low porosity and low permeability, hydraulic fracturing is a necessary means for industrial exploitation of shale gas. In this study, aiming at the problem of reservoir damage in the process of hydraulic fracturing of shale gas reservoir, a physical simulation method of slickwater fracturing fluid flow in shale core has been established. The change laws of physical parameters of the shale were quantified after slickwater fracturing fluid filtrating into it. The main factors affecting physical parameters of shale matrix around fractures were found out in the process of fracturing, shut-in, and flowback of slickwater fracturing fluid. The results show that after treated by slickwater fracturing fluid, the wettability of shale becomes more uniform in distribution (the water contact angles from 43° to 48°). In the fracturing filtration zone, the damage rate of fracturing fluid to shale porosity is 6.4%-42.0%. Low differential pressure flowback can reduce the damage of the shale, and prolonging the time of shut-in has no obvious effect on the damage to porosity. After 0.3 d (imbibition stability time), the damage of fracturing fluid to shale permeability is basically stable (55.9%). Permeability damage is mainly caused by residue of the fracturing fluid in large pores and bound water in small pores. Analysis of weights of all fracturing parameters shows that flowback differential pressure has the largest influence weight on shale porosity (51.4%), and well shut-in time has the largest influence weight on shale permeability (62.7%). Therefore, in the production process, it is suggested to properly reduce the backflow differential pressure and moderately shorten the well shut-in time.

1. Introduction

Shale gas is growing rapidly in production and has gradually become a major contributor to natural gas production in the world. In 2021, the global shale gas production was about $8000 \times 10^8\,m^3$, accounting for more than 20% of the total natural gas production. As a principal type of unconventional oil and gas resources, the economically viable development of shale gas at large scale is an important revolution in the global energy field, which has far-reaching significance for the sustainable development of clean energy.

Shale gas in China is bounty and has broad prospects. But most of shale gas fields in China are distributed in mountainous areas, making them difficult to exploit and high in investment costs. At present, China's shale gas industrial development adopts the approach of "horizontal well + large-scale hydraulic fracturing" [1, 2]. After the completion of hydraulic fracturing, shale gas wells are usually shut-in, and after shut-in for some time, the wells are opened to allow the fracturing fluid in the formation to flow back. However, in the process of fracturing, a large amount of fracturing fluid is often lost and retained in the shale formations, resulting in very low flowback rates. The flowback efficiency of Barnett and Eagle Ford is 20%, while the flowback efficiency of Haynesville shale in Pennsylvania is 5%-45%, respectively [3]. The fracturing fluid retained in the pores under the effect of filtration would have an impact on the physical properties of shale reservoir matrix and further affects the productivity [4, 5] of gas wells. On the one hand, fracturing fluid residues may block the pore throats, which has a negative impact on the porosity and permeability of shale matrix; on the other hand, shale would

swell and has microfractures induced when contacting with foreign fluids with large salinity differences, which has a positive impact on the porosity and permeability of shale gas reservoir [6–8]. In conventional sandstone gas reservoirs, the entry of fracturing fluid can cause reservoir damage, and the backflow of fracturing fluid should be accelerated as much as possible to achieve a higher backflow rate. The field results of shale gas reservoir show that the production effect is better by means of shut-in the well for a period of time and pressure control at the wellhead [9, 10]. The relevant research results indicate that due to the high content of clay minerals in shale, microfractures will occur in the shale after the invasion of fracturing fluid. At the same time, the entry of the liquid phase will change the occurrence environment of shale gas, which will accelerate the desorption and flow of shale gas [11, 12]. The relevant molecular simulation results show that invading water will merge with shale gas to form water-soluble gas, which promotes shale gas migration and leads to a decrease in flowback rate [13, 14]. Lin et al.'s research shows that the increase in pore area after hydration is related to the type of clay contained in shale. There is a strong correlation between the content of illite montmorillonite in the mixed layer and the increase in small and mesoporous volume. And the increase in illite content and micropore volume is the same [15]. The research results of rock mechanics show that fracturing fluid causes shale hydration and rock strength reduction, and the proppant is more likely to be embedded, resulting in a decrease in conductivity of artificial fracture [16]. Zolfaghari et al.'s research shows that the higher the clay content, the greater the cation exchange capacity, which will lead to an increase in the imbibition amount of the fracturing fluid. The dissolution of minerals in shale and the microcracks caused by hydration can lead to an increase of permeability in the early stage of hydration [17]. Roshan et al.'s research shows that mineral dissolution and particle detachment result in mass loss and an increase in porosity during the self-absorption process of shale. The main reasons for quality loss are shale self-absorption rate and temperature [18]. The research of shale hydration on the embedding of proppants and fracture conductivity indicates that shale hydration will reduce elastic modulus of shale. The embedding depth of proppant in shale increases after the action of slippery water without antiswelling agent under the same closure stress conditions. The embedding depth of proppant is linearly related to the closure stress of shale reservoirs [19, 20]. To date, the understanding of the influence of slickwater fracturing fluid on the porosity and permeability of shale reservoir is still limited, and it is necessary to further explore the influence of slickwater fracturing fluid on the physical parameters of shale around fractures in different processes.

In this work, in light of reservoir damage caused by hydraulic fracturing development in Longmaxi shale gas reservoir in Sichuan Basin, a physical simulation method of slickwater fracturing flow in shale core was worked out. Different fracturing processes and production regimes were simulated to find out the influence of fracturing fluid filtrating into formation on shale reservoir physical properties. The multiple linear regression method was used to systematically analyze the main factors affecting the physical parameters of near-fracture shale matrix in the process of fracturing-shut in-flowback. The results of this study can provide an important theoretical basis for the hydraulic fracturing development of shale gas reservoirs.

2. Experiments

2.1. Experimental Materials. Shale samples in the experiments were taken from Longmaxi Formation in YC area, Sichuan Basin. At a burial depth of 4300-4550 m and a temperature of 96°C, the reservoir was fractured at the pressure of 62.1-73.5 MPa. The porosity and permeability of a large number of core samples were measured with helium porosimeter (PMI-100, Yineng, Beijing, China) and pulse decay permeameter (Smart-Perm II, Tal-Rocky Tech System Ltd., Canada), and the specific values are shown in Table 1.

The river water near the well site used to prepare the fracturing fluid has a salinity of 256.8 mg/L and a pH value of 7.2-7.5. The fracturing fluid used in the experiments was the same slickwater fracturing fluid used in the field, and its formula is 0.025% drag reducer CT 5-12, 0.26% cleanup additive CT 1-20 B, and 99.71% river water.

2.2. Tests of Basic Properties of the Slickwater Fracturing Fluid and Shale. The rheological properties and surface tension of the slickwater fracturing fluid were evaluated by HAAKE MARS 60 Rheometer and Teclis Tracker HTHP interfacial rheometer, respectively.

Wettability test of the shale samples followed the steps as follows: the shale core was cut into 5 mm thick slices and dried in an oven at 100°C for 24 h. Visual contact angle measuring instrument (SDC-350, Sindin, China) was used to measure the contact angles of the shale slices. After the shale slices were soaked in the slickwater fracturing fluid for 24 h, the contact angles of them were measured again. The micromorphology and mineral composition of the shale slices were tested by SEM-XRD (Sig300, ZEISS, Germany) after thin sections were obtained by wire cutting.

2.3. Modeling and Evaluation of Fracturing Fluid Flow in Shale Core. The modeling of the slickwater fracturing fluid flow in the shale core followed the steps as follows: (1) The modeling experimental apparatus of fracturing fluid flow in shale core as shown in Figure 1 was built and checked for air tightness. (2) The shale core was put into the core holder under the confining pressure of 9.895 MPa, according to the relevant requirements in the evaluation standard of Chinese water-based fracturing fluid (NB/T 14003.3-2017). (3) The temperature of the experimental apparatus was raised to 96°C, the injection pressure was set at 6.895 MPa according to the relevant requirements in the evaluation standard of Chinese water-based fracturing fluid, and the slickwater fracturing fluid was injected into the shale core in static filtration mode. (4) CH_4 was pumped into the intermediate container by a gas booster pump, and after the well was shut-in for a period of time, the flowback process of fracturing fluid in the field was modeled by reverse CH_4 flooding. (5) After the experiment, the core was dried in an oven at

Table 1: Core parameters.

Core no.	Length (mm)	Diameter (mm)	Permeability (10^{-3} mD)	Porosity (%)
1	25.03	24.98	3.769	4.338
2	24.64	25.10	3.681	5.095
3	24.66	25.05	4.242	4.882
4	24.27	25.11	3.799	4.372
5	25.00	25.01	4.034	4.643
6	24.80	24.97	4.811	5.523
7	25.21	25.04	3.273	4.102
8	24.67	25.09	3.463	4.039
9	25.93	25.20	4.319	6.711
10	25.02	24.98	3.522	4.269
11	24.67	25.09	3.463	3.823
12	24.81	24.95	3.035	6.164
13	25.22	25.17	4.098	6.401
14	25.29	25.22	3.715	3.162
15	25.35	25.01	3.643	4.795

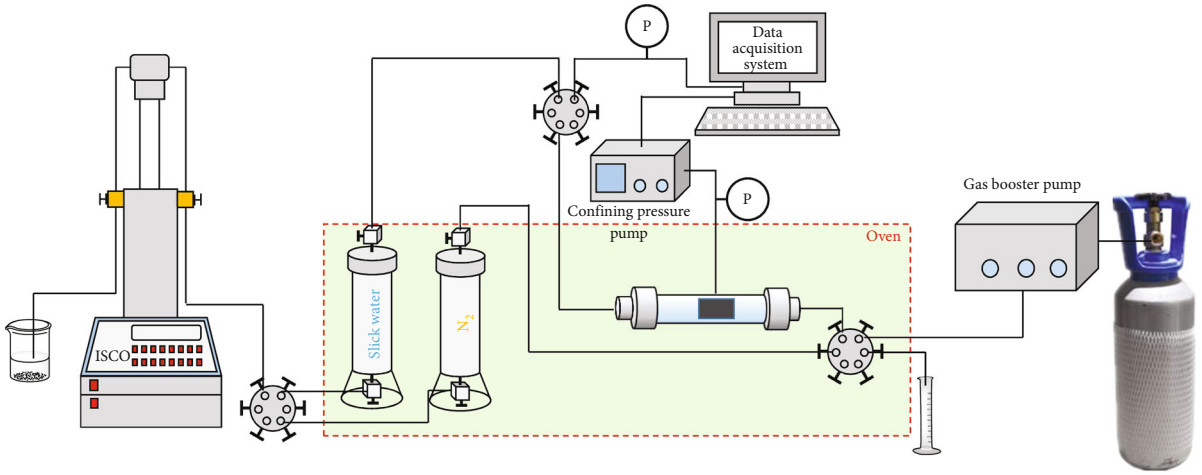

Figure 1: Experimental apparatus modeling fracturing fluid flow.

100°C for 24 h. (6) The porosity and permeability of the shale sample after reaction with slickwater fracturing fluid were measured by a porosimeter and a pulse permeameter.

3. Results and Discussion

3.1. Basic Properties of the Slickwater Fracturing Fluid. The test results of rheological properties of the slickwater fracturing fluid are shown in Figure 2. Slickwater fracturing fluid is a kind of viscoelastic fluid, which shows thinning characteristic under shear and decreases in viscosity with the increase of shear rate. The viscosity of the slickwater fracturing fluid in this study was 1.9 mPa·s at 170 s^{-1}, which meets the oil industry standard of less than 5 mPa·s.

In the hydraulic fracturing process, the cleanup additive concentration in the fracturing fluid is often fine-tuned according to the needs on site. In this work, based on the 0.025% concentration of drag reducer in the slickwater fracturing fluid, the surface tension of slickwater fracturing fluid with different concentration of cleanup additive was examined. The experimental results are shown in Figure 3. The gas-liquid surface tension of the slickwater fracturing fluid decreases with the increase of the concentration of the cleanup additive. When the concentration of cleanup additive is 0.26%, the gas-liquid surface tension reduced to 27.57 mN/m, which met the field requirements [21]. Therefore, the optimal concentration of cleanup additive was 0.26%, which was used in the subsequent experiments.

3.2. Effect of Slickwater Fracturing Fluid on Core Wettability. The wettability of the shale cores before and after treated by the slickwater fracturing fluid was evaluated by a visual contact angle measuring instrument, and the experimental results are shown in Figure 4. The shale cores had a wide range of original wettability, with wetting angles between 22° and 42°. The microscopic morphology and mineral analysis of the shale samples of two lithologies (Figure 5) show that the shale samples before/after imbibition have a certain

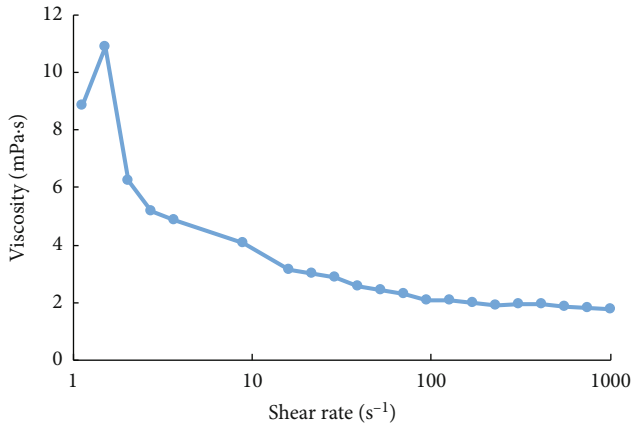

Figure 2: Relationship between viscosity of the slickwater fracturing fluid and shear rate.

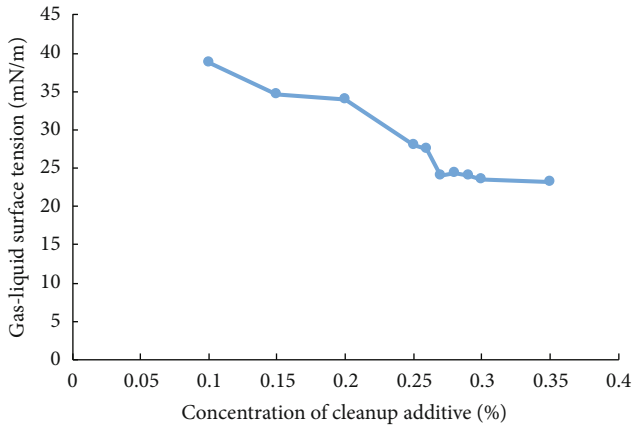

Figure 3: The curve of gas-liquid surface tension vs. concentration of cleanup additive of the fracturing fluid.

degree of local heterogeneity and have stronger hydrophilicity in parts with concentrated quartz, calcite, and dolomite. After treated by the slickwater fracturing fluid, the shale cores became relatively uniform in wettability, with wetting angles from 43° to 48°. Related literature shows that small molecule or polymer in fracturing fluids can adsorb on the surface of shale pore throats, especially the small molecule with cationic structure. The surface wettability of shale after contact fracturing fluids is basically consistent, which is also very consistent with our experimental results [22]. The experimental results show that the slickwater fracturing fluid can change the wettability of shale surface effectively, and shale samples swept by the fracturing fluid will reduce in wettability difference.

3.3. Effects of Slickwater Fracturing Fluid on Porosity and Permeability of Shale Cores

3.3.1. Shut-In Time. Five core samples with similar physical properties and the same slickwater fracturing fluid were selected to carry out flow modeling experiments to find out the effects of different well shut-in time (0, 0.1 d, 0.3 d, 0.5 d, and 1.0 d) on the physical parameters of shale matrix. In the experiments, the pressure at the outlet was the atmospheric pressure, and the differential pressure was fixed at 3.0 MPa. The experimental results are shown in Figures 6 and 7. According to the previous study [23, 24], the imbibition stability time of the shale is about 8 h, and the imbibition stability time of the core is "d." With the increase of well shut-in time, the decline rate of porosity hardly changed, and the decline range of core porosity was 35.2%-42.0%. After shale samples are treated by slickwater fracturing fluid, some residue in the slickwater fracturing fluid is retained in the pore throats of the shale samples and occupies a proportion of the pore throat volume, resulting in a decrease of porosity. Under different well shut-in durations, the decline rate of core porosity hardly changed. This is because the slickwater fracturing fluid migrates to the porous medium under the action of capillary force during the well shut-in, and the retained residue volume is relatively stable, so the porosity does not change much.

Figure 7 shows that the decline rate of permeability changes from 25.1% to 61.8% before 0.3 d and then became stable after 0.3 d. When the well shut-in time is short (<0.3 d), the core rapidly absorbs water and expands and cracks, so fracturing fluid has a positive impact on shale permeability, resulting in a small decline rate of permeability. With the increase of shut-in time, on the one hand, the more fully the fracturing fluid filtrates into the core, the more bound water exists in the core matrix, which leads to the decrease of permeability; on the other hand, the hydration and swelling of clay minerals in shale become more significant, which leads to the decrease of matrix pore throat size, thus the increase of permeability reduction rate. After 0.3 d, the bound water content and clay hydration tend to be stable, and the decline rate of permeability tends stable.

3.3.2. Backflow Differential Pressure. Four cores with similar physical properties and the same slickwater fracturing fluid were taken to do modeling experiments, respectively. Under the same filtration and well shut-in conditions (well shut-in for 8 h), the effects of different pressure differentials (1.0 MPa, 3.0 MPa, 5.0 MPa, and 7.0 MPa) on shale porosity were investigated by fixing the outlet pressure at atmospheric pressure during backflow. The experimental results are shown in Figure 8. With the increase of backflow differential pressure, the decline rate of shale porosity gradually changes significantly, and decrease rate remains stable at 32.8% after 3.0 MPa. When the backflow differential pressure is low, the gas flow is small, and the fingering phenomenon is not significant, so the liquid is easier to flow back, and the amount of slickwater fracturing fluid left in the reservoir is smaller. In contrast, at higher backflow differential pressure, the gas fingering phenomenon is significant, and gas is more likely to break through from the connected large pores, resulting in drop of sweep efficiency of the gas to the slickwater fracturing fluid. At the same time, the gas flow is larger, and the vapor pressure of the liquid reduces, so the water evaporates more quickly [25, 26], and the polymer in the slickwater fracturing fluid would lose the water environment (Figure 9), adsorb on pore walls, and block throats, thus making the porosity loss increase.

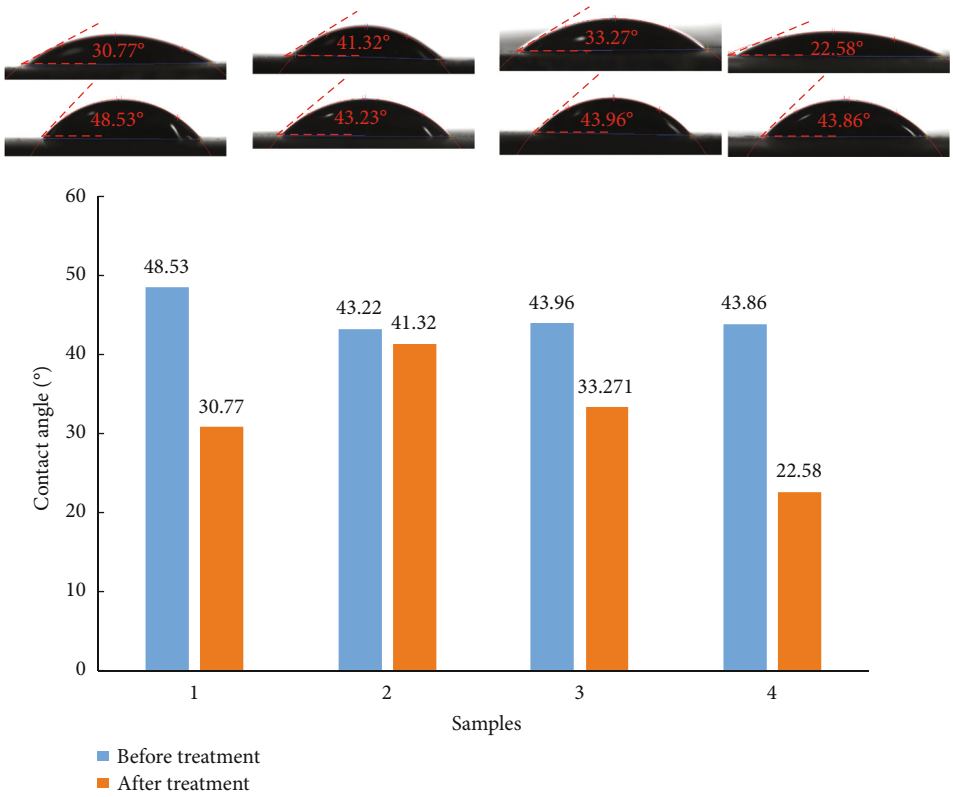

Figure 4: Surface wettability of core samples before and after treated by slickwater fracturing fluid.

Figure 10 shows that with the increase of the backflow differential pressure, the shale matrix permeability decreases by 70.6%-80.1%, the permeability decrease rate hardly changes, and the backflow pressure has little effect on the shale permeability. The decrease rate of shale permeability is mainly affected by the shut-in time, but the flowback pressure difference has little effect. The main reason is that before backflow, shale has reached the imbibition stability time, and the bound water in shale has become stable. In the backflow process, only the movable water in the flow channel can be returned, and the bound water cannot be returned, so the decline rate of shale permeability is almost unchanged.

3.3.3. Effect of the Backflow Outlet Pressure. Flow modeling experiments were carried out on 5 cores with similar physical properties and the same slickwater fracturing fluid under the same conditions of filtration, shut-in (8 h), and 3.0 MPa of flowback differential pressure to find out the effects of different outlet pressures (0 MPa, 1.0 MPa, 3.0 MPa, 5.0 MPa, and 10.0 MPa) on the physical parameters of shale matrix. The experimental results are shown in Figure 11. With the increase of back pressure, the porosity decrease rate drops rapidly from 35.8% to 15.6% first and then tends stable. In the backflow process, with the increase of environmental pressure (the average of injection pressure and outlet pressure), the stress on the core increases, and the internal structure of the core is prone to be damaged; the formation of fractures makes the shale porosity increase; on the other hand, the residual of slickwater fracturing fluid leads to the decline of porosity. When the pressure at the outlet is low, no fractures are formed in the core, and the residual hydraulic fracturing fluid leads to a significant decrease in shale porosity. With the increase of the pressure at the backflow outlet, the shale structure is destroyed, resulting in a significant decrease in core porosity. When the ambient pressure rises to a certain degree, the volume of gas increases, the stress acting on the core gradually stabilizes, and the porosity decline rate tends stable.

Figure 12 shows that with the increase of the pressure at the backflow outlet, the permeability shows a trend of rapid increase and then decrease. In the backflow process, with the increase of pressure at the backflow outlet, the stress acting on the core increases, and the internal structure of the core is prone to be damaged under the dual effects of hydration and environmental pressure, and the formation of penetrating fractures can even make the permeability of shale matrix increase by 1.58-2.97 times. When the outlet pressure increases to a certain level, the density of the backflow gas increases, and the stress on the core gradually stabilizes, and the trend of hydration cracking can be inhibited under stable environmental pressure, so that the internal structure of the core is not prone to damage, and thus, the decline rate of shale permeability is significant.

3.4. Analysis of Factors Affecting Shale Porosity and Permeability. SPSS 26.0 was used as a data analysis tool to conduct multiple linear regression analysis to find out the effects of well shut-in time, backflow differential pressure,

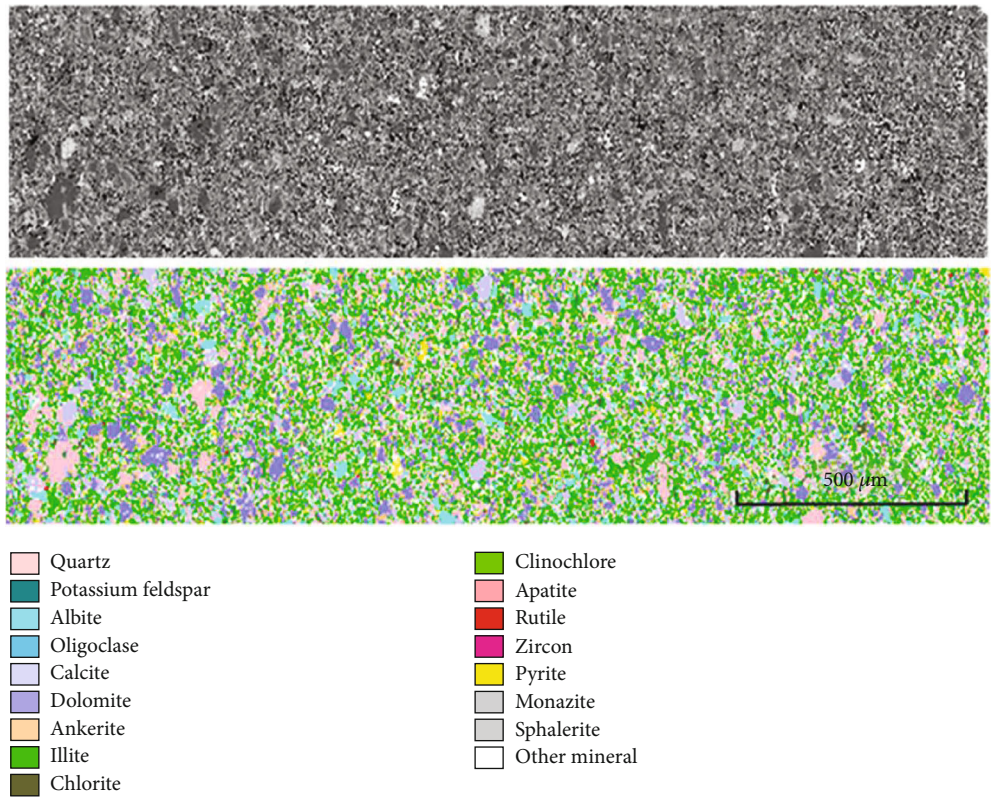

(a)

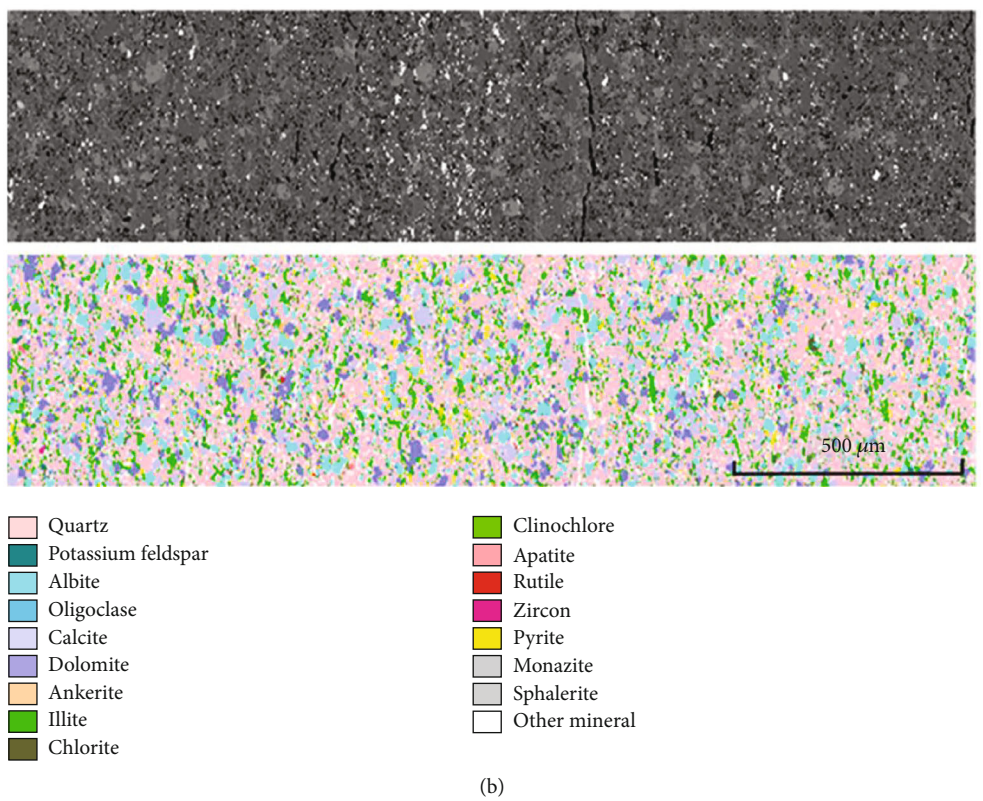

(b)

Figure 5: Micromorphology and mineral composition distribution of shale samples.

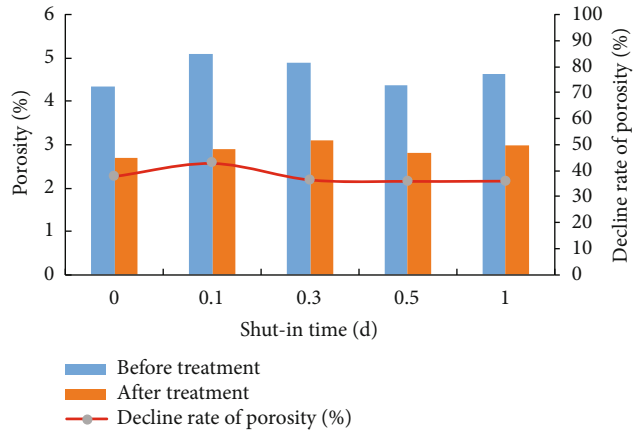

Figure 6: Influence of different well shut-in durations on shale matrix porosity.

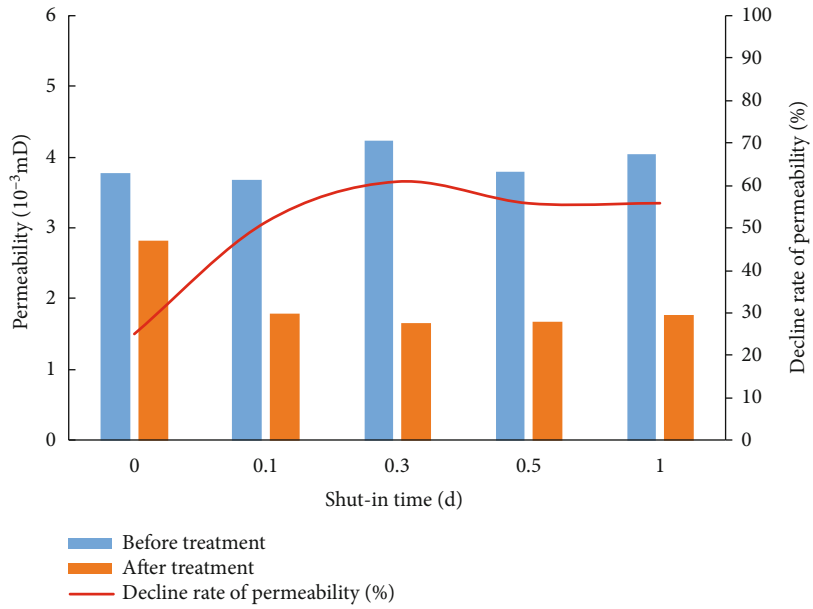

Figure 7: Influence of different well shut-in durations on shale permeability.

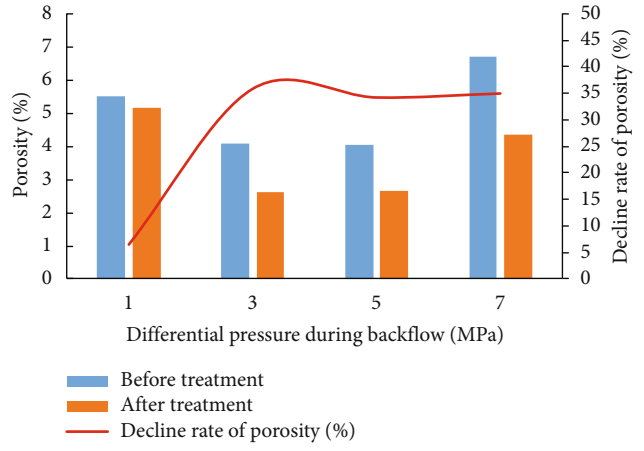

Figure 8: Effect of backflow differential pressure on shale porosity.

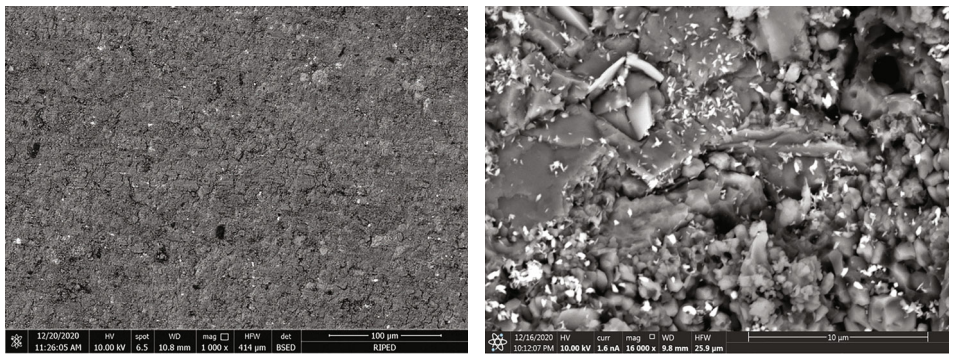

Figure 9: Microscopic morphology with different magnifications of shale after fracturing fluid imbibition.

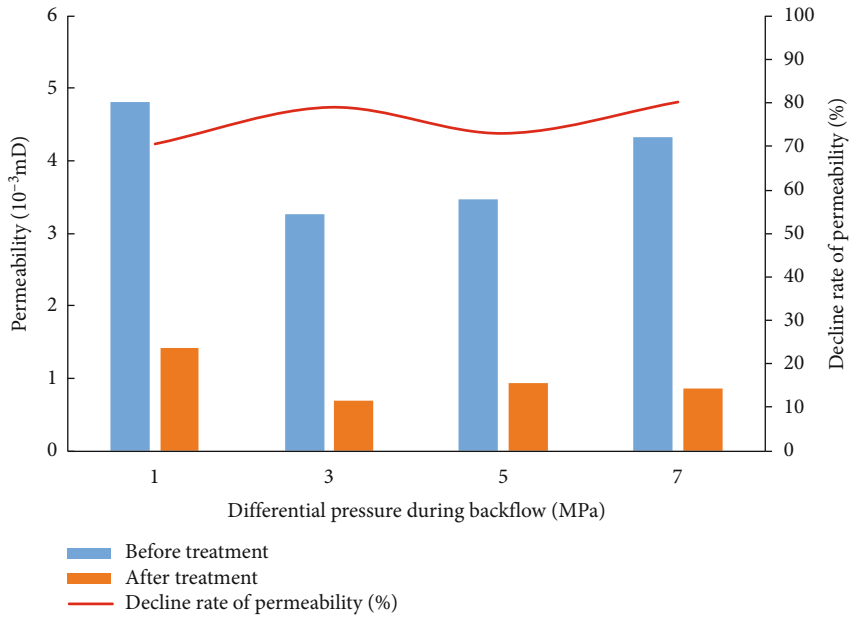

Figure 10: Effect of flowback differential pressure on shale permeability.

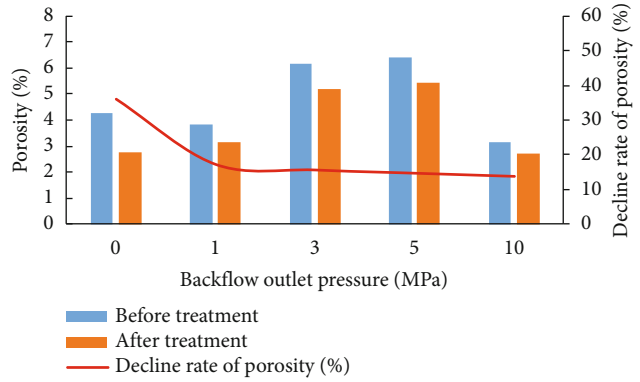

Figure 11: Effects of different backflow outlet pressures on shale porosity.

and backflow outlet pressure on shale porosity and permeability and work out the weights of these factors [27].

3.4.1. Analysis of Factors Influencing Shale Porosity. Multiple linear regression was used to process the data, and then, the weights of different influencing factors were calculated according to the proportion of each factor in the regression equation to clarify the influence degrees of different factors on shale porosity. The correlation coefficients of the factors in the multiple linear regression equation of shale porosity and the correlation analysis of the factors are shown in Tables 2 and 3.

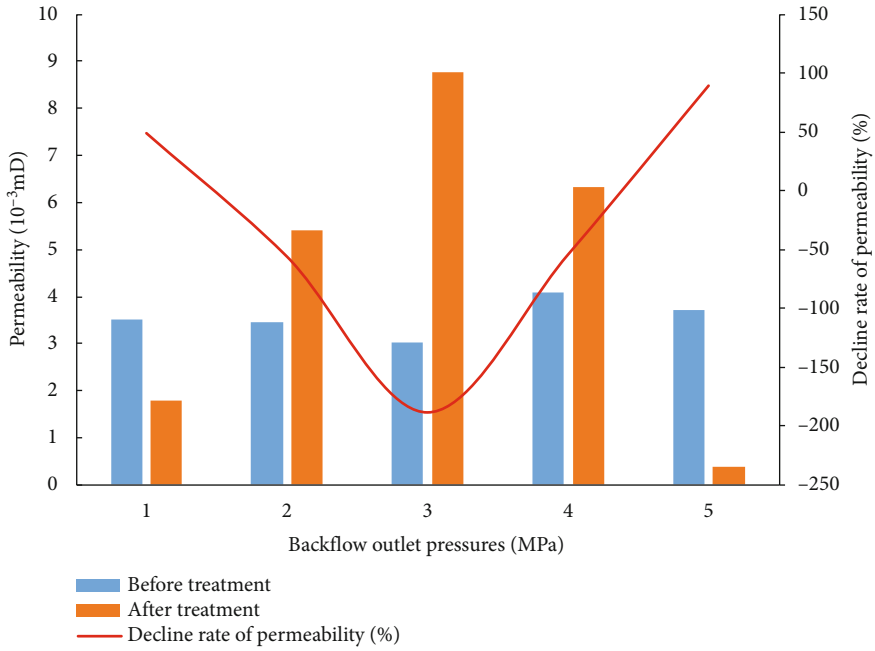

Figure 12: Effects of different backflow outlet pressures on shale permeability.

Table 2: Correlation coefficients of the influencing factors with shale porosity.

		Permeability decline rate	Shut-in time	Backflow outlet pressures	Differential pressure during backflow
Pearson correlation	Rate of porosity decline	1.000	-0.069	-0.120	-0.242
	Shut-in time	-0.069	1.000	-0.152	-0.097
	Backflow outlet pressure	-0.120	-0.152	1.000	0.069
	Differential pressure during backflow	-0.242	-0.097	0.069	1.000
Significance (single tail)	Rate of porosity decline	/	0.365	0.275	0.112
	Shut-in time	0.365	/	0.225	0.315
	Backflow outlet pressure	0.275	0.225	/	0.366
	Backflow differential pressure	0.112	0.315	0.366	/
Number of cases	Rate of porosity decline	27	27	27	27
	Shut-in time	27	27	27	27
	Backflow outlet pressure	27	27	27	27
	Differential pressure during backflow	27	27	27	27

Table 3: Regression coefficients of the factors influencing shale porosity.

Model	Non-normalized coefficient		Normalized coefficient		
	B	Standard error	Beta	t	Significance
(Constant)	0.417	0.216		1.931	0.066
Shut-in time	-0.057	0.153	-0.078	0.372	0.713
Backflow outlet pressure	-0.012	0.017	-0.141	-0.688	0.498
Differential pressure during backflow	-0.066	0.058	-0.232	-1.142	0.266

Table 4: Correlation coefficients of the influencing factors with shale permeability.

		Permeability decline rate	Shut-in time	Backflow outlet pressures	Backflow differential pressure
Pearson correlation	Permeability decline rate	1.000	-0.128	0.050	-0.019
	Shut-in time	-0.128	1.000	-0.152	-0.097
	Backflow outlet pressure	0.050	-0.152	1.000	0.069
	Differential pressure during backflow	0.019	-0.097	0.069	1.000
Significance (single tail)	Permeability decline rate	/	0.262	0.402	0.463
	Shut-in time	0.262	/	0.225	0.315
	Backflow outlet pressure	0.402	0.225	/	0.366
	Backflow differential pressure	0.463	0.315	0.366	/
Number of cases	Permeability decline rate	27	27	27	27
	Shut-in time	27	27	27	27
	Backflow outlet pressure	27	27	27	27
	Backflow differential pressure	27	27	27	27

Table 5: Regression coefficients of factors influencing shale permeability.

Model	Non-normalized coefficient		Normalized coefficient		
	B	Standard error	Beta	t	Significance
(Constant)	0.859	0.935	/	0.918	0.369
Shut-in time	-0.451	0.660	-0.148	-0.683	0.502
Backflow outlet pressure	0.017	0.075	0.047	0.220	0.828
Differential pressure during backflow	-0.049	0.250	-0.041	-0.195	0.847

Normalization is to remove the dimension, so the relative importance of the variables can be reflected. Here, the goal of normalization is only to compare the relative effects of multiple independent variables on the dependent variable, so the normalized regression coefficient is used. Usually, the significance value should be less than 0.05 to be called significant; that is, the linear regression is valid [28–30]. Because of operation errors and uncontrollable physical and chemical factors in the actual operation process, it is difficult to make the experimental results reach the ideal state. It can be concluded that the factors in descending order of influence on porosity are differential pressure during backflow, backflow outlet pressure, and shut-in time, and further, the weights of the variable factors were calculated as follows:

$$\begin{aligned}&\text{Weight of differential pressure during backflow}\\&= \frac{0.232}{0.078 + 0.141 + 0.232} \times 100\% = 51.4\%,\\&\text{Weight of backflow outlet pressure}\\&= \frac{0.141}{0.078 + 0.141 + 0.232} \times 100\% = 31.3\%,\\&\text{Weight of shut-in time}\\&= \frac{0.078}{0.078 + 0.141 + 0.232} \times 100\% = 17.3\%.\end{aligned} \tag{1}$$

3.4.2. Analysis of Factors Influencing Shale Permeability. By the same method, the correlation of each factor and the coefficient of each factor in the multiple regression equation of permeability can be obtained, as shown in Tables 4 and 5.

Comprehensive analysis shows that the factors in descending order of influence on permeability are shut-in time, backflow outlet pressure, and differential pressure during backflow. The weights of the variable factors were further calculated as follows:

$$\begin{aligned}&\text{Weight of shut-in time}\\&= \frac{0.148}{0.148 + 0.047 + 0.041} \times 100\% = 62.7\%,\\&\text{Weight of backflow outlet pressure}\\&= \frac{0.047}{0.148 + 0.047 + 0.041} \times 100\% = 19.9\%,\\&\text{Weight of differential pressure during backflow}\\&= \frac{0.041}{0.148 + 0.047 + 0.041} \times 100\% = 17.4\%.\end{aligned} \tag{2}$$

4. Conclusions

In this study, aiming at the shale gas reservoir damage caused by hydraulic fracturing fluid, a physical simulation method of fracturing fluid flow in shale core was worked

out to analyze the influence of slickwater hydraulic fracturing fluid on the physical properties of near-fracture shale matrix in the fracturing-shut-in-backflow process systematically. The following conclusions have been drawn:

(1) Slickwater fracturing fluid (0.025% CT 5-12 + 0.26% CT 1-20 B) has a viscosity of 1.99 mPa·s at the shear rate of 170 s^{-1} and gas-liquid surface tension decreasing to 27.57 mN/m. After treated by the slickwater fracturing fluid, the shale cores become more uniform in wettability, with contact angles between 43° and 48°

(2) During the fracturing filtration period, the damage of slickwater fracturing fluid to shale porosity is between 6.4% and 42%. Low differential pressure backflow can reduce the damage to shale porosity, and prolonging the shut-in time has little effect on porosity damage

(3) After shut-in of 0.3 d (stable imbibition time), the damage of the slickwater fracturing fluid to the permeability is basically stable (up to 55.9%). The damage to permeability is mainly caused by residues of slickwater fracturing fluid in large pores and irreducible water in small pores

(4) The influence weight of backflow differential pressure on shale porosity is the largest (51.4%), and the influence weight of shut-in time on shale permeability is the largest (62.7%), so the backflow differential pressure should be properly lowered and the shut-in time should be moderately shortened during shale gas production

Data Availability

Authenticity of Laboratory and On-Site Data. All data used in this study can be obtained by contacting the corresponding author, through the following email addresses: jwliu_petrochina@163.com and liujw_2022@petrochina.com.cn.

Conflicts of Interest

The authors declare that they have no conflicts of interest.

Authors' Contributions

Jiawei Liu was responsible for the original draft of the manuscript and the formulation or evolution of overarching research goals. Xuefeng Yang was responsible for the development or design of methodology and supervision of the experiments. Shengxian Zhao reviewed and edited the initial draft. Yue Yang was responsible for the curation of the experimental data. Shan Huang was responsible for the formal analysis and investigation. Lieyan Cao was responsible for the formal analysis and methodology. Jiajun Li was responsible for the formal analysis and methodology. Jian Zhang was responsible for the validation and supervision of the experiments.

Acknowledgments

This work was financially supported by the Major Science and Technology Projects of PetroChina (2023ZZ21) and the Southwest Oil and Gas Field Branch Technology Project (20230312-02). The research is supported by the PetroChina Southwest Oil & Gasfield Company.

References

[1] C. Sun, H. Nie, W. Dang et al., "Shale gas exploration and development in China: current status, geological challenges, and future directions," *Energy & Fuels*, vol. 35, no. 8, pp. 6359–6379, 2021.

[2] J. Guo, L. Yang, and S. Wang, "Adsorption damage and control measures of slick-water fracturing fluid in shale reservoirs," *Petroleum Exploration and Development*, vol. 45, no. 2, pp. 336–342, 2018.

[3] L. You, N. Zhang, Y. Kang, J. Xu, Q. Chen, and Y. Zhou, "Zero flowback rate of hydraulic fracturing fluid in shale gas reservoirs: concept, feasibility, and significance," *Energy & Fuels*, vol. 35, no. 7, pp. 5671–5682, 2021.

[4] X. Liu, Y. Zhuang, L. Liang, and J. Xiong, "Investigation on the influence of water-shale interaction on stress sensitivity of organic-rich shale," *Geofluids*, vol. 2019, Article ID 2598727, 13 pages, 2019.

[5] N. Farah, D. Ding, and Y. Wu, "Simulation of the impact of fracturing-fluid-induced formation damage in shale gas reservoirs," *SPE Reservoir Evaluation & Engineering*, vol. 20, no. 3, pp. 532–546, 2017.

[6] L. You, B. Xie, J. Yang, and B. Yang, "Mechanism of fracture damage induced by fracturing fluid flowback in shale gas reservoirs," *Natural Gas Industry B*, vol. 6, no. 4, pp. 366–373, 2019.

[7] Y. Zhou, L. You, Y. Kang, C. Jia, and B. Xiao, "Influencing factors and application of spontaneous imbibition of fracturing fluids in lacustrine and marine shale gas reservoir," *Energy & Fuels*, vol. 36, no. 7, pp. 3606–3618, 2022.

[8] J. Shao, L. You, Y. Kang, M. Chen, and J. Tian, "Salinity of flowback fracturing fluid in shale reservoir and its reservoir damage: experimental and field study," *Journal of Petroleum Science and Engineering*, vol. 211, article 110217, 2022.

[9] C. Xu, Y. Kang, Z. You, and M. Chen, "Review on formation damage mechanisms and processes in shale gas reservoir: known and to be known," *Journal of Natural Gas Science and Engineering*, vol. 36, pp. 1208–1219, 2016.

[10] S. Huang, X. Ma, J. Wu, X. Ma, R. Yong, and T. Wu, "Transient interporosity flow in shale/tight oil reservoirs: model and application," *ACS Omega*, vol. 7, no. 17, pp. 14746–14755, 2022.

[11] S. Wu, J. Wu, Y. Liu, J. Zhang, B. Zhong, and D. Liu, "Lattice Boltzmann modeling of the coupled imbibition-flowback behavior in a 3D shale pore structure under reservoir condition," *Frontiers in Earth Science*, vol. 11, article 1138938, 2023.

[12] A. Minardi, A. Ferrari, R. Ewy, and L. Laloui, "The impact of the volumetric swelling behavior on the water uptake of gas shale," *Journal of Natural Gas Science and Engineering*, vol. 49, pp. 132–144, 2018.

[13] J. Wu, Y. Di, P. Li, P. Li, J. Zhang, and D. Liang, "Numerical simulation of choke size optimization in a shale gas well," *Geofluids*, vol. 2022, Article ID 2197001, 12 pages, 2022.

[14] S. Huang, W. Li, J. Wu, H. Zhang, and Y. Luo, "A study of the mechanism of nonuniform production rate in shale gas based on nonradioactive gas tracer technology," *Energy Science & Engineering*, vol. 8, no. 7, pp. 2648–2658, 2020.

[15] H. Lin, X. Sun, Y. Yuan, X. Lai, H. Qu, and C. Luo, "Experimental investigation on the dynamic volume changes of varied-size pores during shale hydration," *Journal of Natural Gas Science and Engineering*, vol. 101, article 104506, 2022.

[16] T. Lee, D. Jeong, Y. So, D. Park, M. Baek, and J. Choe, "Integrated workflow of geomechanics, hydraulic fracturing, and reservoir simulation for production estimation of a shale gas reservoir," *Geofluids*, vol. 2021, Article ID 8856070, 17 pages, 2021.

[17] A. Zolfaghari, H. Dehghanpour, M. Noel, and D. Bearinger, "Laboratory and field analysis of flowback water from gas shales," *Journal of Unconventional Oil and Gas Resources*, vol. 14, pp. 113–127, 2016.

[18] H. Roshan, S. Ehsani, C. Marjo, M. Andersen, and R. Acworth, "Mechanisms of water adsorption into partially saturated fractured shales: an experimental study," *Fuel*, vol. 159, pp. 628–637, 2015.

[19] T. Huang, L. Cao, J. Cai, and P. Xu, "Experimental investigation on rock structure and chemical properties of hard brittle shale under different drilling fluids," *Journal of Petroleum Science and Engineering*, vol. 181, pp. 106185–106189, 2019.

[20] Q. Wang, C. Lyu, and D. R. Cole, "Effects of hydration on fractures and shale permeability under different confining pressures: an experimental study," *Journal of Petroleum Science and Engineering*, vol. 176, pp. 745–753, 2019.

[21] S. Cheng, P. Huang, K. Wang, K. Wang, and Z. Chen, "Comprehensive modeling of multiple transport mechanisms in shale gas reservoir production," *Fuel*, vol. 277, article 118159, 2020.

[22] Y. Hu, C. Zhao, J. Zhou, Q. Wang, D. Gao, and C. Fu, "Mechanisms of fracturing fluid spontaneous imbibition behavior in shale reservoir: a review," *Journal of Natural Gas Science and Engineering*, vol. 82, article 103498, 2020.

[23] X. Ding, Q. You, J. Wu et al., "Hydration characteristics and mechanism study of artificial fracture surface in illite rich shale gas reservoir: a case study of Longmaxi formation shale in Yongchuan District," *Energy Reports*, vol. 9, pp. 4174–4186, 2023.

[24] J. Liu, L. Li, Z. Xu, J. Chen, and C. Dai, "Self-growing hydrogel particles with applications for reservoir control: growth behaviors and influencing factors," *The Journal of Physical Chemistry B*, vol. 125, no. 34, pp. 9870–9878, 2021.

[25] Y. Sun, B. Bai, and M. Wei, "Microfracture and surfactant impact on linear cocurrent brine imbibition in gas-saturated shale," *Energy & Fuels*, vol. 29, no. 3, pp. 1438–1446, 2015.

[26] T. Ma, C. Yang, P. Chen, X. Wang, and Y. Guo, "On the damage constitutive model for hydrated shale using CT scanning technology," *Journal of Natural Gas Science and Engineering*, vol. 28, pp. 204–214, 2016.

[27] Y. Kang, J. She, H. Zhang, L. You, Y. Yu, and M. Song, "Alkali erosion of shale by high-pH fluid: reaction kinetic behaviors and engineering responses," *Journal of Natural Gas Science and Engineering*, vol. 29, pp. 201–210, 2016.

[28] H. Dehghanpour, Q. Lan, Y. Saeed, and Z. Qi, "Spontaneous imbibition of brine and oil in gas shales: effect of water adsorption and resulting microfractures," *Energy & Fuels*, vol. 27, no. 6, pp. 3039–3049, 2013.

[29] S. Bagci and S. Stolyarov, "Flowback production optimization for choke size management strategies in unconventional wells," in *SPE Annual Technical Conference and Exhibition*, Calgary, Alberta, Canada, 2019.

[30] Z. Sun, H. Zhang, Z. Wei et al., "Effects of slick water fracturing fluid on pore structure and adsorption characteristics of shale reservoir rocks," *Journal of Natural Gas Science and Engineering*, vol. 51, pp. 27–36, 2018.